

Naval Research Laboratory

Washington, DC 20375-5000

DTIC ELECTRIC



NRL Memorandum Report 6215

AD-A196 348

Theoretical Prediction of Ripple-Load Effect on Stress-Corrosion Cracking

G. R. YODER, P. S. PAO, AND R. A. BAYLES

*Mechanics of Materials Branch
Materials Science and Technology Division*

May 31 1988

DTIC
ELECTE
JUN 15 1988
S D
CD

88 6 11 3 2 0

Approved for public release; distribution unlimited.

REPORT DOCUMENTATION PAGE				Form Approved OMB No 0704-0188	
1a. REPORT SECURITY CLASSIFICATION UNCLASSIFIED		1b. RESTRICTIVE MARKINGS			
2a. SECURITY CLASSIFICATION AUTHORITY		3. DISTRIBUTION / AVAILABILITY OF REPORT Approved for public release; distribution unlimited.			
2b. DECLASSIFICATION / DOWNGRADING SCHEDULE					
4. PERFORMING ORGANIZATION REPORT NUMBER(S) NRL Memorandum Report 6215		5. MONITORING ORGANIZATION REPORT NUMBER(S)			
6a. NAME OF PERFORMING ORGANIZATION Naval Research Laboratory		6b. OFFICE SYMBOL (If applicable) Code 6384	7a. NAME OF MONITORING ORGANIZATION Office of Naval Research		
6c. ADDRESS (City, State, and ZIP Code) Washington, DC 20375-5000		7b. ADDRESS (City, State, and ZIP Code) Arlington, VA 22217-5000			
8a. NAME OF FUNDING / SPONSORING ORGANIZATION		8b. OFFICE SYMBOL (If applicable)	9. PROCUREMENT INSTRUMENT IDENTIFICATION NUMBER		
8c. ADDRESS (City, State, and ZIP Code)		10. SOURCE OF FUNDING NUMBERS			
		PROGRAM ELEMENT NO. 61153N	PROJECT NO. RR022-08-01	TASK NO.	WORK UNIT ACCESSION NO.
11. TITLE (Include Security Classification) (U) Theoretical Prediction of Ripple-Load Effect on Stress-Corrosion Cracking					
12. PERSONAL AUTHOR(S) Yoder, George R., Pao, Peter S. and Bayles, R. A.					
13a. TYPE OF REPORT		13b. TIME COVERED FROM _____ TO _____	14. DATE OF REPORT (Year, Month, Day) 1988 May 31		15. PAGE COUNT 17
16. SUPPLEMENTARY NOTATION					
17. COSATI CODES			18. SUBJECT TERMS (Continue on reverse if necessary and identify by block number)		
FIELD	GROUP	SUB-GROUP	Stress-corrosion cracking, High stress ratio. <i>JES</i> ←		
			Corrosion fatigue		
			Ripple-load cracking		
19. ABSTRACT (Continue on reverse if necessary and identify by block number) The ripple-load effect (RLE) is a perplexing phenomenon in which the threshold stress-intensity factor ($K_{I_{SCC}}$) for stress-corrosion cracking (SCC) appears to be severely degraded — at least in some cases, if the constant load condition characteristic of SCC is perturbed by superposition of a small-amplitude cyclic load. In this study, a theoretical framework has been developed to predict the conditions required for a material to exhibit a RLE in a marine environment — and the extent of such degradation. Insofar as a framework for the RLE necessarily involves the interface between SCC and corrosion fatigue (CF), the model presented herein derives from concepts and descriptors used in SCC and CF characterization. Thus, analysis begins with consideration of the relationship between the small amplitude stress-intensity range associated with ripple loading, ΔK , the high stress-ratio conditions, $R > 0.90$, the threshold for CF crack growth, ΔK_{th} , the maximum stress-intensity factor in the loading cycle, K_{max} . (Continues) — >					
20. DISTRIBUTION / AVAILABILITY OF ABSTRACT <input checked="" type="checkbox"/> UNCLASSIFIED/UNLIMITED <input type="checkbox"/> SAME AS RPT <input type="checkbox"/> DTIC USERS			21. ABSTRACT SECURITY CLASSIFICATION UNCLASSIFIED		
22a. NAME OF RESPONSIBLE INDIVIDUAL George R. Yoder			22b. TELEPHONE (Include Area Code) (202) 767-3571	22c. OFFICE SYMBOL Code 6384	

19. ABSTRACT (Continued)

and K_{Isc} . The results are expressed in terms of critical conditions required for the RLE to occur, as well as the predictive equation for the maximum degradation that would be anticipated — or, alternatively, the threshold level of stress-intensity factor below which ripple-load cracking would not occur. Moreover, through numerical integration of CF crack growth rate data, it is shown that the time-to-failure curves associated with ripple-load degradation can be predicted for a specific combination of material/structure and loading conditions.

CONTENTS

INTRODUCTION	1
ANALYSIS OF RIPPLE-LOAD EFFECT (RLE)	2
A. Critical Conditions (for susceptibility)	2
B. Maximum Extent of Degradation	3
C. Quantitative Prediction of Time-to-failure (t_f) Curves	4
DISCUSSION	6
CONCLUSIONS	7
ACKNOWLEDGMENTS	7
REFERENCES	8

Accession For	
NTIS CRA&I	<input checked="" type="checkbox"/>
DTIC TAB	<input type="checkbox"/>
Unannounced	<input type="checkbox"/>
Justification	
By	
Distribution/	
Availability Codes	
Dist	Avail and/or Special
A-1	



THEORETICAL PREDICTION OF RIPPLE-LOAD EFFECT ON STRESS-CORROSION CRACKING

INTRODUCTION

For a structural material which contains a crack or crack-like defect, the resistance to stress-corrosion cracking is normally evaluated in terms of the fracture mechanics parameter, $K_{I_{SCC}}$, the threshold stress-intensity factor below which fracture will not occur. The measurement of $K_{I_{SCC}}$ and its application to design of structures for the marine environment commonly presume sustained or constant load conditions. However, recent work⁽¹⁻⁶⁾ has demonstrated that with the superposition of a very small amplitude cyclic load (or "ripple load"), fracture can occur in some cases at stress-intensity levels much less than $K_{I_{SCC}}$. An extensive literature survey on such ripple-load effects was recently prepared, which cited several examples from both ferrous and nonferrous alloy systems⁽⁷⁾. Applications in the real world -- including many in the Navy --- rarely involve an absolutely constant load condition, but are far more apt to involve the superposition of relatively small amplitude load perturbations. Thus, the implications of the ripple-load effect (RLE) may be quite serious. Indeed, ripple-load cracking has been reported to occur at stress-intensity levels as much as 60 per cent below $K_{I_{SCC}}$, as in the case of a 5Ni-Cr-Mo-V steel⁽⁶⁾, as illustrated in Fig. 1a. On the other hand, it does not appear from the literature that all ferrous alloys exhibit similar levels of ripple-load degradation. In fact, wide disparities have been reported --- to the point of complete absence of a RLE in some cases, as in the case of an AISI 4340 steel⁽⁶⁾, cf. Fig. 1b --- for reasons which have remained obscure. The origin of the RLE is even more confused by recent evidence that an increase in time-to-failure may be caused by ripple loading, in the case of a 3Ni-Cr-Mo-V steel⁽⁶⁾.

The purpose of this work is to develop the theoretical framework required for prediction of the RLE. First of all, definition is sought of the critical conditions required for a material to exhibit a RLE in the marine environment. Secondly, quantitative prediction is desired of the maximum extent of degradation by the RLE, relative to $K_{I_{SCC}}$ --- i.e. a threshold below which ripple-load cracking will not occur. And finally, the quantitative

prediction of time-to-failure curves associated with ripple-load cracking is sought, for a given combination of material/structure and loading conditions. The desired framework necessarily involves the interface between SCC and corrosion-fatigue (CF) behavior. Ripple-load cracking has been approached as an extreme case of CF crack growth behavior. Thus, the analysis begins with consideration of the relationship between the small amplitude stress-intensity range associated with ripple loading, ΔK , the high stress-ratio conditions, $R \geq 0.90$, the threshold for CF crack growth, ΔK_{th} , the maximum stress-intensity factor in the loading cycle, K_{max} , and K_{Isc} .

ANALYSIS OF RIPPLE-LOAD EFFECT (RLE)

A. Critical Conditions (for susceptibility)

To define the critical conditions required for a material to exhibit a RLE in marine environment, consider first of all the nature of the interface between stress-corrosion cracking and corrosion fatigue, as represented in the schematics of Fig. 2. In Fig. 2a, the SCC resistance is indicated by the "static" loading curve, wherein the level of K represents the initial value of stress-intensity factor associated with a precracked specimen (structure) which is subjected to a constant load. Here, K_{Isc} represents a threshold level below which fracture will not occur. However, if this constant load is superposed with a "ripple" or small-amplitude cyclic load --- as in the schematic of Fig. 2b, then for a material exhibiting susceptibility to the RLE, cracking resistance appears to be degraded to levels significantly below K_{Isc} , as in Fig. 2a. There, the K -level plotted for the "ripple" curve is actually K_{max}^{RL} , the maximum level of K in the ripple-load cycle, cf. Fig. 2b. If the RLE is defined as degradation relative to the "static" K_{Isc} threshold, then the first condition for the RLE can be expressed as:

$$K_{max}^{RL} \leq K_{Isc} \quad (1)$$

With the treatment of ripple-load cracking as an extreme case of very high stress ratio*, CF crack growth, then with reference to Fig. 2b, this

*In the context of a "ripple" or small amplitude cyclic load, the stress ratio is generally presumed to be $R \geq 0.90$, although such a stipulation does not affect the generality of the treatment offered herein. With regard to notation, the superscript "RL" will be used to denote ripple loading, and the subscript "th" to denote threshold.

condition can be represented in terms of stress-intensity range,

$$\Delta K^{RL} \leq (1-R) * K_{Isc} \quad (1a)$$

where R is the stress ratio ($K_{min}:K_{max}$) and $\Delta K = K_{max} - K_{min}$. Now the resistance of a material to CF crack growth is normally reported in terms of fatigue crack growth rate (da/dN) as a function of ΔK , as shown in Fig. 2c. The lower limit of the ΔK spectrum is defined by ΔK_{th} , the threshold level below which cracks will not propagate (while the upper bound is controlled by the fracture toughness). Consequently, cracks cannot propagate to failure under ripple-loading for any material unless this second condition is also met:

$$\Delta K^{RL} \geq \Delta K_{th} \quad (2)$$

Or, equivalently, the threshold level of K --- below which ripple-load cracking will not occur, is given by:

$$K_{max}^{RL} |_{th} = \frac{\Delta K_{th}}{1-R} \quad (2a)$$

Consequently, if conditions (1) and (2) are combined, it can be stated that a material will exhibit a susceptibility to the RLE if and only if:

$$\frac{\Delta K_{th}}{1-R} \leq K_{max}^{RL} \leq K_{Isc} \quad (3)$$

Or, equivalently,

$$\Delta K_{th} \leq \Delta K^{RL} \leq (1-R) * K_{Isc} \quad (3a)$$

B. Maximum Extent of Degradation

Relation (3) thus defines a "window" for which the RLE would be anticipated --- as sketched in Fig. 3a. If one considers the differential

between the threshold for ripple-load cracking ($K_{max|th}^{RL}$) and K_{IscC} , then the maximum amount of degradation attributable to the RLE is given by:

$$\% \text{ degradation}^{RL} = \left[1 - \frac{\Delta K_{th}}{K_{IscC} * (1-R)} \right] * 100 \quad (4)$$

On the other hand, if conditions of relation (3) are not met, a material will not exhibit susceptibility to the RLE --- as illustrated in Fig. 3b, since**

$$\frac{\Delta K_{th}}{1-R} > K_{IscC} \quad (5)$$

C. Quantitative Prediction of Time-to-failure (t_f) Curves

Though the typical logarithmic CF crack-growth rate curve may well exhibit a more complex shape than shown in the schematic of Fig. 2c, nevertheless, it can be approximated in piecewise fashion with power-law segments,

$$\frac{da}{dN} = C_j * (\Delta K)^{m_j} \quad (6)$$

Or,

$$dN = \frac{da}{C_j * (\Delta K)^{m_j}} \quad (6a)$$

Thus, the total number of cycles to propagate a crack can be estimated

**This statement and the preceding are contingent, of course, upon definition of the RLE as degradation relative to the K_{IscC} threshold. If, however, attention were to be focused on cracking behavior above K_{IscC} , then it is important to recognize that for levels of K_{max} in excess of K_{IscC} in the "susceptible" case --- or in excess of $K_{max|th}^{RL}$ in the "nonsusceptible" case, "ripple" or cyclic loading at $R \geq 0.90$ will definitely affect the time-to-failure (t_f). For a given geometry, reductions in t_f would be anticipated from levels associated with "static" loading, in accord with the superposition model of CF⁽⁸⁾. These reduced levels of t_f can still be computed using the framework described in the following section.

from the piecewise integration (over j segments) as:

$$N_p = \sum_j \int_{(a_i)_j}^{(a_f)_j} \frac{da}{C_j * (1-R)^{m_j} * K_{max}^{m_j}} \quad (7)$$

where $(a_i)_j$ and $(a_f)_j$ are initial and final crack sizes relative to the j th segment. Of course, for the initial segment of the integration, a_i is the starting flaw (crack) size in the actual specimen or structure. On the other hand, for the final segment, a_f is the flaw (crack) size at failure.

Thus, a_f can be obtained from knowledge of the fracture toughness --- K_{Ic} in the case of plane strain crack tip constraint. (However, if the point of general yielding is attained prior to fracture instability, then the integration should be truncated with an a_f associated with such point.) Since stress-intensity factor can be expressed in general as:

$$K = P * f(a,Q) \quad (8)$$

where P is load and $f(a,Q)$ is a function of crack length (a) and structural geometry (Q), then equation (7) can be rewritten as:

$$N_p = \sum_j \int_{(a_i)_j}^{(a_f)_j} \frac{da}{C_j [(1-R) * P_{max} * f(a,Q)]^{m_j}} \quad (7a)$$

Now time-to-failure is simply given by:

$$t_f = \frac{N_p}{v} \quad (9)$$

where v is the cyclic frequency. Thus, finally, t_f can be estimated as:

$$t_f = \frac{1}{v} \sum_j \int_{(a_i)_j}^{(a_f)_j} \frac{da}{C_j [(1-R) * P_{max} * f(a,Q)]^{m_j}} \quad (10)$$

Though in certain cases equation (8) is sufficiently simple to permit direct integration of equation (10) --- such as in the case of a center-cracked

tension panel, in general, a numerical integration of equation (10) will facilitate computation.

DISCUSSION

It is useful to elaborate somewhat on a number of points related to the predictive methodology offered in this paper. First of all, it is appropriate to ask the question: what material properties tend to promote the high levels of $K_{I_{SCC}}$ and low levels of ΔK_{th} which promote the ripple-load degradation indicated by relations (3) or (4)? In general, higher levels of $K_{I_{SCC}}$ tend to be associated with lower yield strength, higher toughness materials⁽⁹⁾. On the other hand, there is evidence that the lower levels of ΔK_{th} are related to smaller grain size or microstructural mean free path dimension --- and higher yield strength^(10,11). Thus, interestingly, it would appear that strength level may play competing roles relative to ripple-load degradation.

Secondly, it is useful to focus further on the parameter, $K_{max|th}^{RL}$, and its relation to $K_{I_{SCC}}$ --- since susceptibility or nonsusceptibility of a material to the RLE depends on whether the level of $K_{I_{SCC}}$ exceeds the term, $\Delta K_{th}/(1-R)$, or not (cf. relation (3) or (5)). Even though the numerator (ΔK_{th}) is a parameter that normally decreases with an increase in R , it is clear that the denominator is a quite potent function of R at the high levels of stress ratio concerned with ripple loading ($R \geq 0.90$). Thus if the term, $\Delta K_{th}/(1-R)$, increases significantly with increased R , it may have the potential to rise from levels less than $K_{I_{SCC}}$ to levels in excess. In this way, theoretically at least, a material may be capable of exhibiting both susceptibility and nonsusceptibility to the RLE, depending on the particular value of R . Thus, it appears that susceptibility to the RLE is not necessarily a material characteristic.

A few words are also in order regarding the time-to-failure curves. It is significant to note that the corrosion-fatigue data required for their prediction, via equation (10), are readily obtained via automated test methods. The framework offered herein thus permits the saving of much greater time and expense associated with experimental determination of such time-to-failure curves, which are geometry dependent. Furthermore, the CF crack growth rate data employed in the predictive framework have the anticipated virtue of geometry independence --- if plane strain crack-tip constraint prevails.

If, however, predictive t_f curves are desired for structures (geometries) exhibiting crack-tip constraint relaxed from the plane strain level, then it would be most appropriate to develop corrosion-fatigue crack-growth rate data for the particular section size of concern. It should be pointed out, though, that geometry-independent CF crack growth rate data (for plane strain) would still offer a useful, conservative estimate of t_f for cases where the constraint is relaxed.

The t_f curves, as indicated by equation (10), are not only geometry dependent, but also frequency dependent. Insofar as some alloys exhibit unusual frequency dependence in their CF crack growth behavior⁽¹²⁾, frequency has the potential to be a significant variable relative to estimates of t_f .

CONCLUSIONS

- A predictive model for the ripple-load effect (RLE) has been developed from concepts and descriptors used in stress-corrosion cracking (SCC) and corrosion-fatigue (CF) characterization.
- Definition has been made of the critical conditions required for the appearance of a RLE.
- A mathematical expression has been developed to describe the maximum extent of RLE degradation, for a specific combination of material/structure and loading conditions.
- Susceptibility to the RLE does not appear to be a material characteristic; rather, if an appropriate value of $K_{I_{SCC}}$ is presumed --- together with a reasonable dependence of ΔK_{th} on R , then a material may theoretically exhibit both susceptibility and nonsusceptibility, depending on the particular level of R .

ACKNOWLEDGMENTS

The support of this work by the Office of Naval Research is gratefully acknowledged (ONR Work Unit No. 4315195). Special thanks are extended to Dr. A. J. Sedriks, ONR Scientific Officer (Corrosion Science), for his continual encouragement.

REFERENCES

1. K. Komai and K. Minoshima, "Influences of Stress Ratios and Cyclic Frequencies on Dynamic SCC Crack Growth in an Al Alloy," Proceedings of the International Congress on Metallic Corrosion, June 3 - 7, 1984, Vol. 1. National Research Council of Canada, Toronto, 1984, pp. 167-173.
2. R. N. Parkins and B. S. Greenwell, "The Interface Between Corrosion Fatigue and Stress-Corrosion Cracking," Metal Science, August/September 1977, pp. 405-413.
3. F. P. Ford and M. Silverman, "The Effect of Loading on Environmentally Controlled Cracking of Sensitized 304 Stainless Steel in High Purity Water," Corrosion-NACE, Vol. 36, No. 11, November 1980, pp. 597-603.
4. J. Avila Mendoza and J. M. Sykes, "The Effect of Low-Frequency Cyclic Stresses on the Initiation of Stress-Corrosion Cracks in X60 Line Pipe Steel in Carbonate Solutions," Corrosion Science, Vol. 23, No. 6, 1983, pp. 547-588.
5. R. R. Fessler and T. J. Barlo, "Threshold-Stress Determination Using Tapered Specimens and Cyclic Stresses," Environment-Sensitive Fracture: Evaluation and Comparison of Test Methods, ASTM STP 821, S. W. Dean, E. N. Pugh, and G. M. Ugiansky, Eds., American Society for Testing and Materials, Philadelphia, 1984, pp. 368-382.
6. T. W. Crooker, J. A. Hauser II and R. A. Bayles, "Ripple-Load Cracking Effects on Stress-Corrosion Cracking in Steels," Proceedings of Third International Conference on Environmental Degradation of Engineering Materials-III, M. R. Louthan, Jr., R. P. McNitt and R. D. Sisson, Jr., Eds., The Pennsylvania State University Press, University Park, PA, 1987, pp. 521-532.
7. T. W. Crooker and J. A. Hauser II, "A Literature Review on the Influence of Small-Amplitude Cyclic Loading on Stress-Corrosion Cracking in Alloys," NRL Memorandum Report 5763, Naval Research Laboratory, Washington DC, April 3, 1986.
8. R. P. Wei and J. D. Landes, "Correlation between Sustained-Load and Fatigue Crack Growth in High Strength Steels", Materials Research and Standards, American Society for Testing and Materials, Philadelphia, PA, Vol. 9, 1969, pp. 25-28.

9. G. Sandoz, "High Strength Steels," Chapter 3 in Stress-Corrosion Cracking in High Strength Steels and in Titanium and Aluminum Alloys, B. F. Brown, editor, U. S. Government Printing Office, Washington, DC, 1972, pp.79-145.
10. G. R. Yoder, L. A. Cooley, and T.W. Crooker, "A Critical Analysis of Grain-Size and Yield-Strength Dependence of Near-Threshold Fatigue Crack Growth in Steels," Fracture Mechanics: Fourteenth Symposium --- Volume 1: Theory and Analysis, ASTM STP 791, J. C. Lewis and G. Sines, Eds., American Society for Testing and Materials, Philadelphia, PA, 1983, pp. 1-348 - 1-365.
11. S. Taira, K. Tanaka, and M. Hoshina, in Fatigue Mechanisms, ASTM STP 675, American Society for Testing and Materials, Philadelphia, PA, 1979, pp. 135-162.
12. G. R. Yoder, L. A. Cooley and T. W. Crooker, "Effects of Microstructure and Frequency on Corrosion-Fatigue Crack Growth in Ti-8Al-1Mo-1V and Ti-6Al-4V," Corrosion Fatigue: Mechanics, Metallurgy, Electrochemistry and Engineering, ASTM STP 801, T. W. Crooker and B. N. Leis, Eds., American Society for Testing and Materials, Philadelphia, PA, 1983, pp. 159-174.

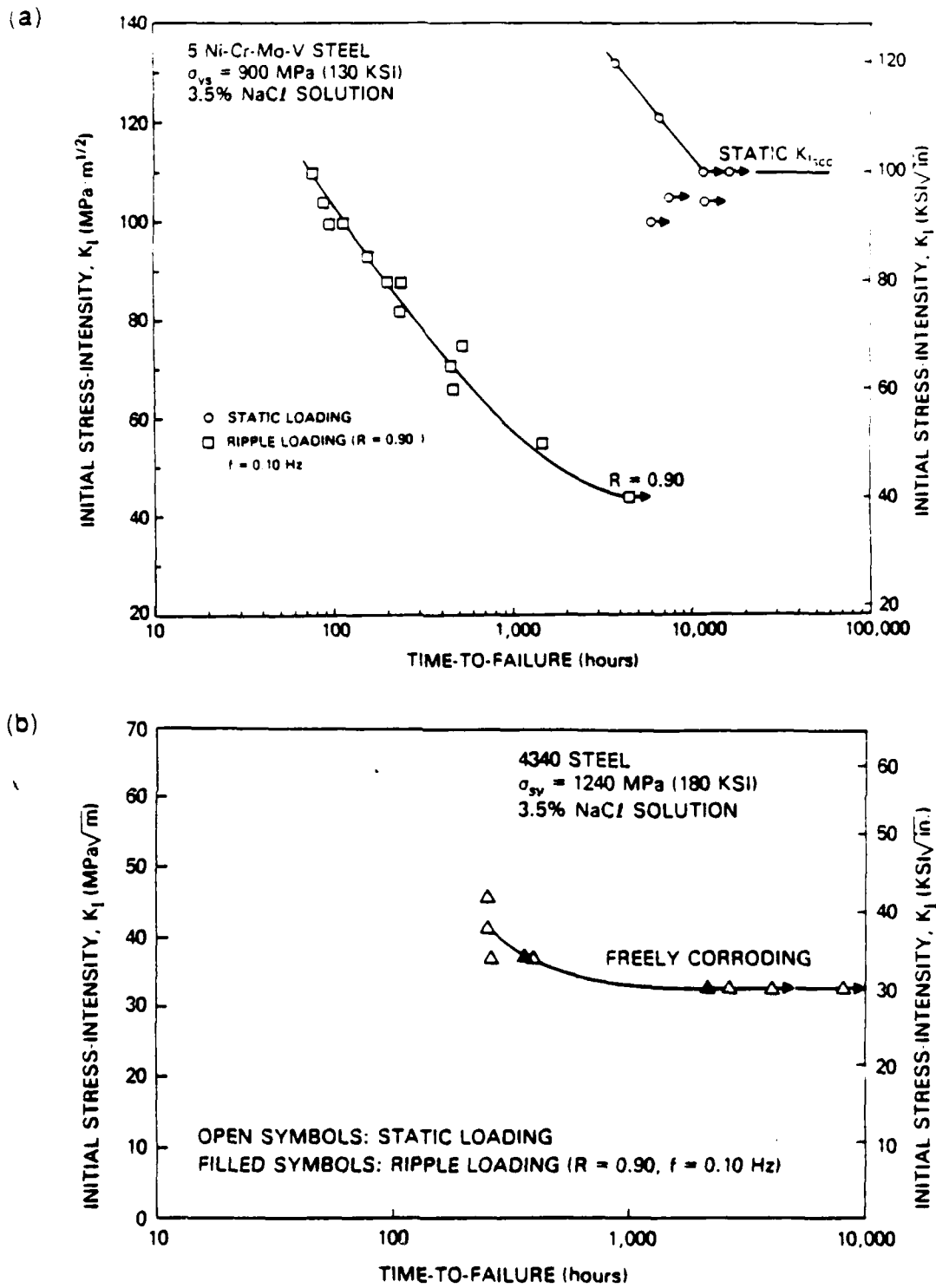


Fig. 1. Susceptibility to ripple-load degradation versus nonsusceptibility in two ferrous alloys cycled at $R=0.90$ in 3.5% NaCl solution. (a) susceptibility in a 5Ni-Cr-Mo-V steel; (b) nonsusceptibility in an AISI 4340 steel.

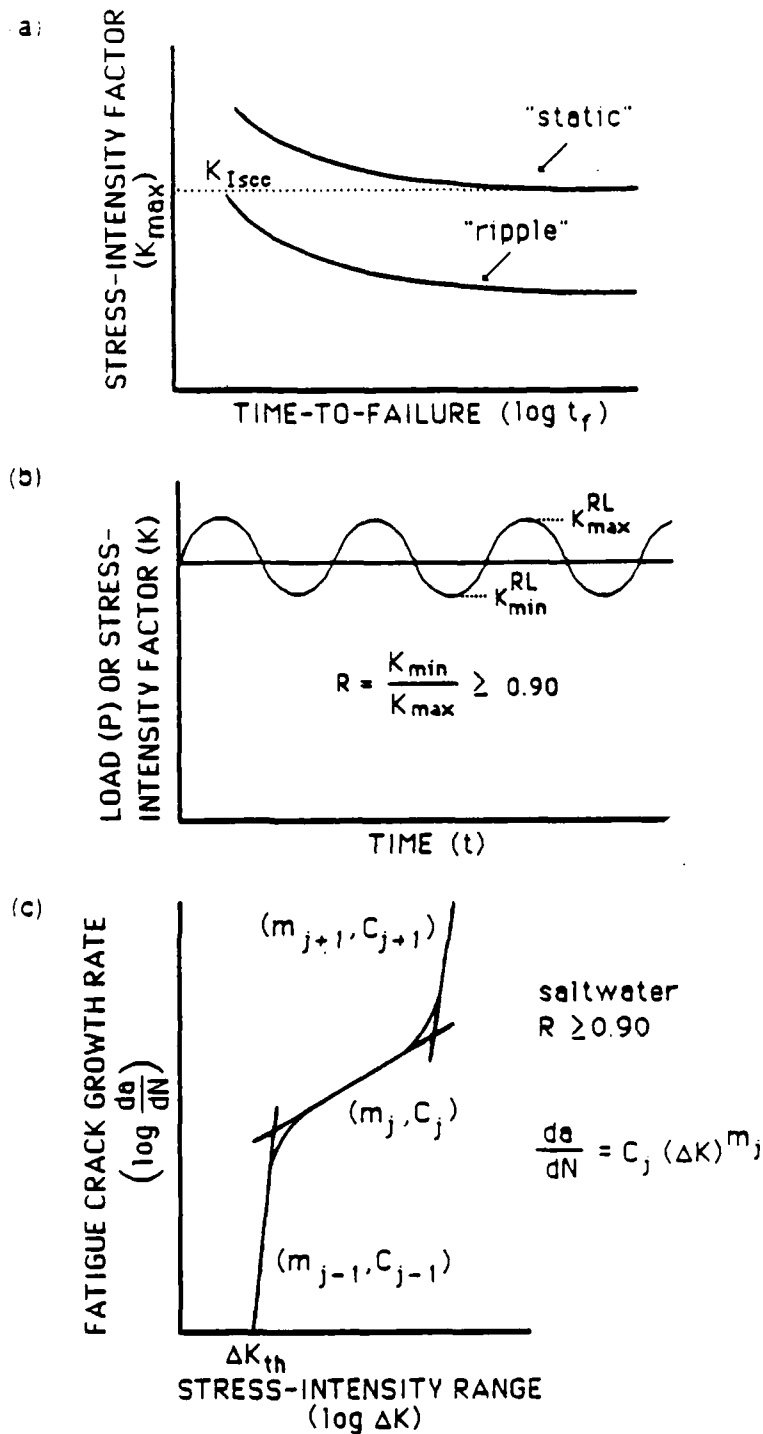
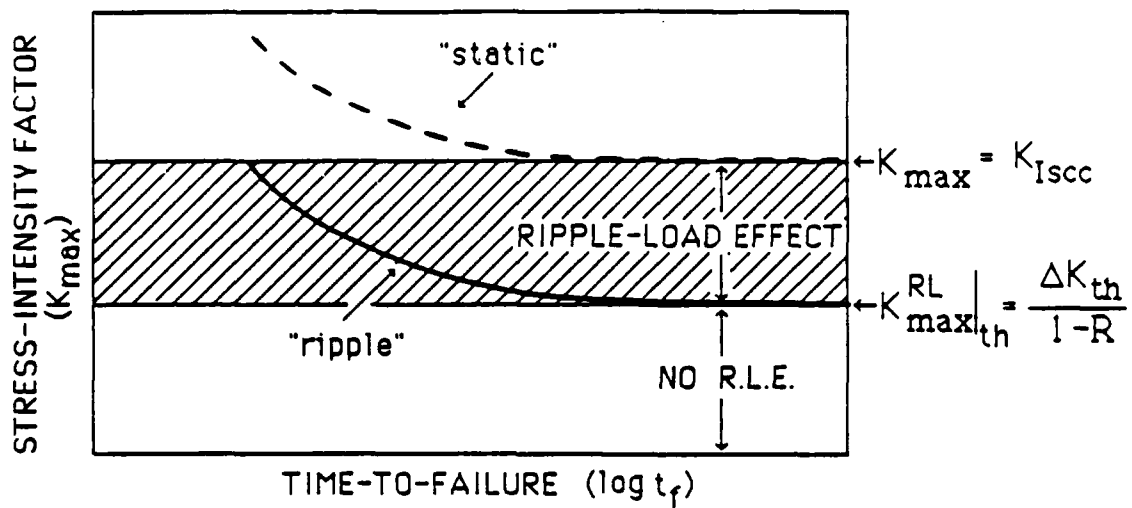


Fig. 2. Schematics on analysis of RLE. (a) "ripple"-load degradation analyzed via K_{max} parameter versus "static" K_{Isc} threshold; cf. text. (b) "ripple" or small amplitude cyclic load superposed on much larger sustained load; stress ratio, $R \geq 0.90$. (c) piecewise analysis of corrosion-fatigue crack growth rate curve via power-law approximation to j^{th} segment.

A. SUSCEPTIBLE CASE



B. NONSUSCEPTIBLE CASE

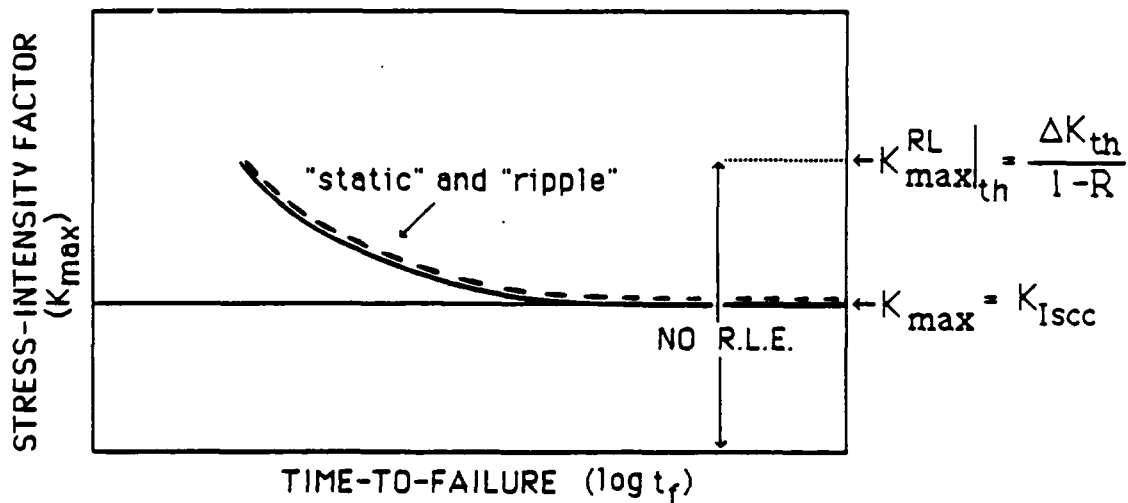


Fig. 3. Illustration of predictions from relation (3); cf. text. (a) susceptibility to RLE. (b) non-susceptibility to ripple-load degradation.